

Deformation Analysis of XILONGCHI Upper Reservoir Using Continuous GPS Data

Liu Hongfei^{a,*} Zhou Xiaohui^a Lizhao^a Deng Liansheng^a

^aSchool of Geodesy and Geomatics, Wuhan University, 129 Luoyu Road, Wuhan 430079, China-
(hfliu,xhzhou)@sgg.whu.edu.cn, lizhao_83@yahoo.com.cn

KEY WORDS: GPS, Deformation Monitoring, Coordinate time series, Short baseline, Annual signal, Multipath, white noise

ABSTRACT:

Long time series from GPS have been the main tool in quantitatively analyzing crustal deformation. Many researchers have illustrated that the secular trend and periodic signals in GPS position time series could explain crustal deformation and its corresponding loading effects. Therefore, continuous GPS data collected from GPS Deformation Monitoring System can be used to obtain deformation properties of reservoir. In this paper we processed continuous GPS observations spanned 20 months from five GPS stations in Xilongchi Reservoir Deformation Monitoring System using DDMS software developed by us, obtained coordinate time series for 4-hour session solution. Then the long-term deformation of the reservoir was determined. Multipath effects were firstly investigated. It is shown that there were little difference between elevation cutoff angle of 15° and 25°. Results from the analysis of time series show that site L022 on the main dam moves north by east 81° at 1.9 mm/yr, while S071, north by east 109° at 2.2mm/yr, L132, north by west 87° at 0.8mm/yr. The rest 2 sites S171, S191 move westward slightly. Besides, all sites exhibit downward movement in various degree, among them L022 on main dam subsiding at the fastest rate of 3.8 mm/yr. Sites L132 (on auxiliary dam), S171, S191, and S071 subside at rates of 1.4 mm/yr, 0.5 mm/yr, 1.0 mm/yr and 0.8mm/yr respectively. All sites, except for L132, show annual variations with an amplitude of ~ 1mm in east component, which suggests a correlation between annual signals and local temperature especially for sites L022 and TN01. Annual signals may be resulted from thermal expansion of the bedrock due to its seasonal characteristic.

1. INTRODUCTION

Global Position System (GPS) is now being used to measure ground deformation at the level of < 1mm (Hill, 2009), while coordinate time series from global solution are the main approach to infer the change in Earth's shape at secular and seasonal timescale, such as due to tectonic motion, glacial isostatic adjustment or hydrological loading (King, 2009). The geophysical parameter derived from long GPS time series is biased at some level by residual systematic error including multipath, antenna phase center variations, unmodeled atmospheric effects, satellite orbit errors, unmodeled solid earth tides and ocean tides. These systematic errors and their propagation mechanism have not been understood yet.

Recent research has highlighted that long-period systematic errors may occur in coordinate time series due to either spurious signal or real movement. Real signal may occur owing to the unmodeled movement such as geophysical loading and thermal expansion of monument, bedrock, etc., while spurious signal may originate from unmodeled long-term signals propagated differently as the satellite constellation changes. Dong *et al.* (2002) found that only ~40% of the observed annual signal in GPS time series could be explained by geophysical surface loading models. There are so many effects are lumped together and termed "errors" in GPS solutions. Therefore it is important that we understand the degree to which such effects can contribute to both time- and space-dependent signal in the GPS time series (Hill, 2009).

While some errors (e.g. atmospheric effects and satellite orbits) would cancel at high degree over shorter intersite distance (less

than 1km) in GPS Deformation Monitoring System, others can not be cancelled, such as multipath, antenna phase center variations. Those errors became obstacles to obtain isolate true displacement. In this paper, we follow the convention of shorter baseline, and focus on the separation of long-term deformation in GPS time series lumped with uncertain multipath effects. GPS observations from Xilongchi upper reservoir during recent 2 years were processed by DDMS software, then the coordinate time series was analyzed by CATS. At last the long-term deformation trend of Xilongchi upper reservoir was determined.

2. GPS DATA PROCESSING

2.1. Data Sets

Stations involved in this article include two reference sites and five sites served as continuous operation stations in the Xilongchi deformation monitoring system, as shown in Figure 1. Two reference sites, named TN02 and TN01, located in the northeast and southeast corner of the reservoir respectively (red triangle), while five continuous sites of L022, S191, S171, L132, S071 (blue triangle) are located around the reservoir, equipped with TRIMBLE NETRS receiver, CHOKE RING antenna (TRM29659.00) for data acquirement 24 hours per day. Distance between above stations ranges from 200m to 600m. The reference sites have good observation condition with no shelter above the elevation of 8 degrees, and are built in a special observation pillar, which is directly anchored on the bedrock. Those 5 continuous monitoring stations are also equipped with CHOKE RING antennas like the reference station, which is beneficial to prohibit the multipath effect and cancel common PCV.

* Hongfei Liu, PhD Students in School of Geodesy and Geomatics, Wuhan University, China, focus on the processing theory of GPS observations and its application in deformation monitoring.

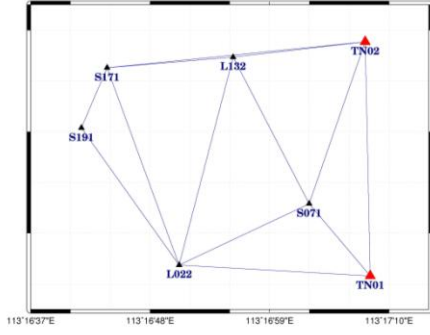


Figure 1. Location of sites served as reference stations and monitoring stations in Xilongchi GPS monitoring system. Sites TN02 and TN01 are reference stations and the other 5 sites are monitoring stations.

2.2. Processing Strategy

We process the GPS observations from September 2009 to May 2011 in this paper. Many errors will either be cancelled or significantly reduced by double-differencing method in DDMS due to the small extent of network. Processing strategy which takes advantage of this feature is as follows: 1) GPS data is processed in 4-hours session solution, namely the normal equation is inverted and parameters are estimated using observations with length of 4 hours, thus we can get six solutions in one day. 2) Position estimates are based on L1 frequency data only since these are a factor ~ 3 more precise than the LC observations. 3) We don't include estimation of zenith delay parameters based on the viewpoint that the troposphere delay is cancelled in double-differenced method over such short baseline. 4) Corrections for ocean tide and solid earth tide is neglected. 5) Satellite orbits were fixed to the coordinates from broadcast ephemeris. The effect of inaccurate orbit can be neglected as well owing to the analysis in the paper (JIANG, 1998). 6) Parameters were estimated in network-solution mode, that is to say, only a group of independent baselines were estimated and the corresponding dual difference ambiguities were fixed to its true integer. 7) Coordinate of TN02 was fixed to the initial coordinate during network adjustment which is previously determined from the global solution with IGS stations nearby. 8) Because of the accordance of antenna's orientation on each station, we use the absolute antenna phase center corrections (PCV) model that is dependent with the elevation only, ignoring the effect of azimuth. 9) We process the same observations with different elevation cut-off angle, respectively by 15° and 25° in order to analyze the effect of multipath based on the cognition that Multipath is more likely to affect signal that arrive at the receiver from low elevation angles and its effects will be modified using a higher elevation cut-off angle.

2.3. Outliers Cleaning

Here we use three criterion for the quality control of the solution results: 1) When processing with DDMS software, the value of nrms namely the square root of chi-square per degree of freedom is an important indicator of data quality, which is usually required to be less than 0.6. In this paper we set the threshold to be 0.4. 2) The solution is removed if any one of the ambiguities is not fixed. 3) For the coordinate series

$\{x_1, x_2, \dots, x_N\}$ of each site, we calculate the second-difference sequence as follows:

$$d_j = 2x_j - (x_{j+1} + x_{j-1}), (j=2,3,4,\dots,N-1) \quad (1)$$

We consider that the second-difference sequence follows Gaussian distributions with an average as \bar{d} , and variance as $\hat{\sigma}_d$. These estimated values can be obtained from the sequence itself. The factor q_j is calculated as follows,

$$q_j = \frac{|d_j - \bar{d}|}{\hat{\sigma}_d} \quad (2)$$

The point with index j is considered as outlier and discarded if $q_j > 2.5$.

3. RESULTS

3.1. Coordinate Time Series

Cleaned coordinate time series after outliers rejection mentioned above is shown in figure 2, where results with 10° elevation cutoff is represented in green dots and the ones with 25° in blue dots. Several stations such as L132 and S191 have time series step marked with red line at a level of several millimetres, which coincide with the events of antenna change. Nearly all stations show obvious displacement in time series (light grey region between two dashed lines in figure 2), especially for the north component with deviation up to 5-10mm, which gradually rebound and remains steady before and after November 15, 2009. According to the comparison with meteorological data, we found a big blizzard swept the region of Xilongchi upper reservoir during that period. One rationale was that snow fell onto the radome and disturbed the instantaneous antenna phase center. Of course we cannot rule out the possibility of deformation due to snow loading. The mechanism requires further studies, which are beyond the scope of this paper. We removed the corresponding points in time series during that period for the following analysis.

Coordinate time series (north, east up) are shown in Figure 2 for all continuous observed stations in Xilongchi system. Broadly speaking, three kinds of feature are apparent in Figure 2. Firstly, all stations except for S071 remain stable and exhibit small displacement over 20 months, after the preliminary impoundment of Xilongchi upper reservoir. The fluctuation of all series are within the range of -3mm~3mm for horizontal component, and -5mm~5mm for radial component respectively. Secondly, some stations exhibit linear motion for several components, among which station L022 reveals obvious movement for east and up direction. These secular trend undoubtedly represents the deformation of located section of reservoir. Meanwhile all stations are descending with different velocities during the same period. Thirdly, several solutions exhibit strong annual variation in each component, with reduced scatter after increasing of elevation cut-off angle. It is obvious that annual signal with low amplitude exists in the east

component even for reference station TN01. In addition, site S071 have steps in time series at several millimeter level for the east component that do not correspond to events.

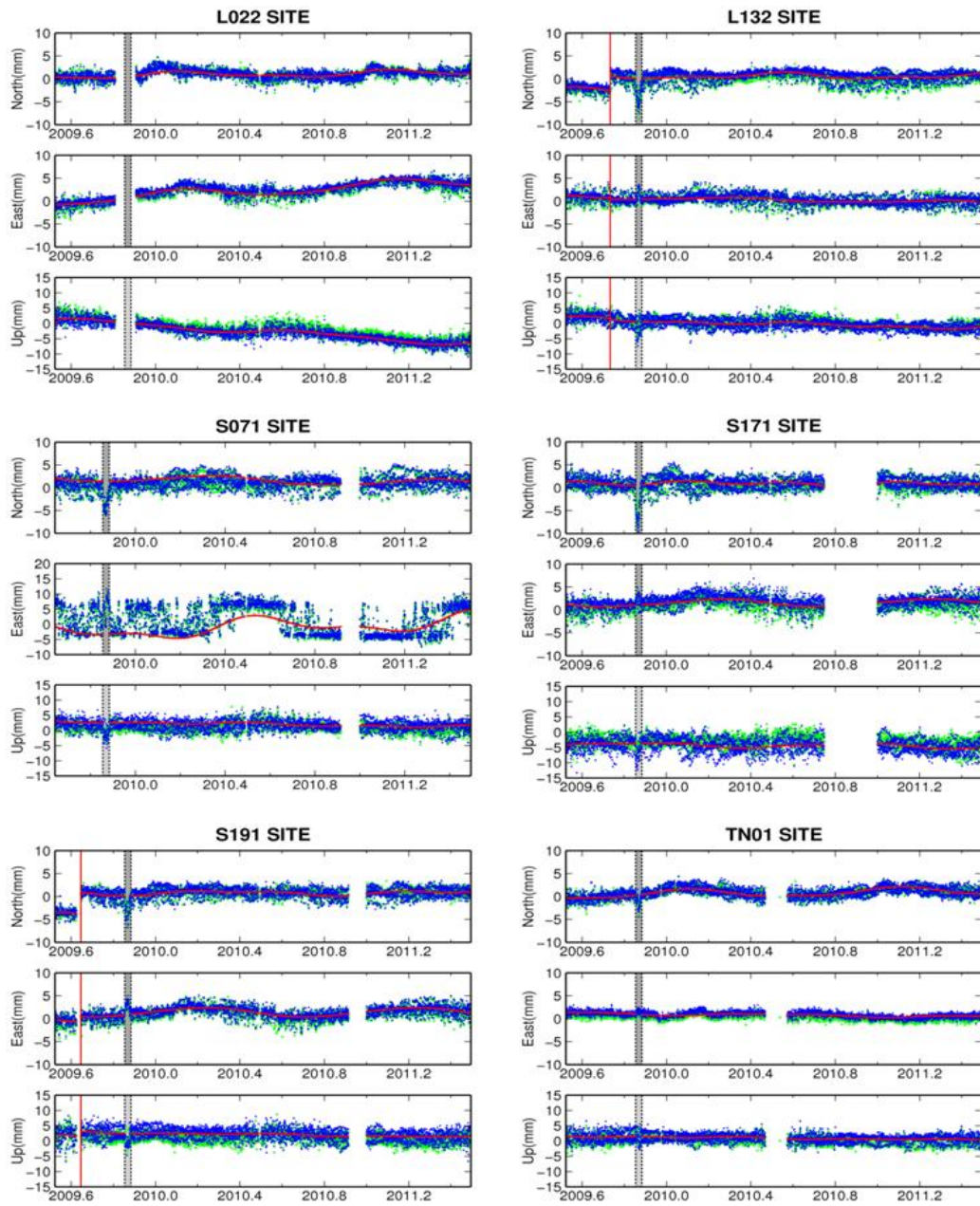


Figure 2. Changes in coordinate time series for the monitoring stations. Blue and green dots are the solution using 15° and 25° cutoff angles, respectively. Red vertical lines represent the step owing to replacement of antenna or receivers, while light grey region between two dashed lines represents the abrupt change during the period of heavy snow. Red lines represent the same data fitted by the model.

station	N (mm)				E (mm)				U (mm)			
	Max	Min	Ave	RMS	Max	Min	Ave	RMS	RMS	Min	Ave	RMS
L022	1.8	-1.4	0.0	0.4	2.0	-0.7	0.3	0.3	3.3	-4.0	-0.6	0.8
L132	2.0	-3.1	0.4	0.3	2.0	-0.8	0.3	0.3	3.6	-6.5	-0.4	1.0
S071	1.5	-2.1	0.1	0.4	1.6	-1.6	0.3	0.3	4.8	-4.7	0.7	1.0
S171	2.9	-3.0	0.4	0.5	2.6	-1.5	0.7	0.5	4.5	-5.2	-1.1	1.8
S191	2.7	-2.7	0.0	0.4	2.7	-0.9	0.3	0.2	4.8	-4.1	1.0	1.0
TN01	1.1	-1.2	0.1	0.4	1.2	-0.5	0.5	0.6	1.4	-1.2	0.5	0.8

Table 1 Statistics of the difference sequence between 15° and 25° Elevation Cutoff Angle Solutions

4. ANALYSIS

4.1. Multipath effect

Some investigations indicate that there exists annual signal in the GPS short-baseline time series. Hill (2009) analyzed a network which has baseline lengths ranging from ~10 m, 100 m and 1 km. Results showed that seasonal cycles occur, with amplitudes of 0.04-0.60mm, even for the horizontal components and even for the shortest baseline. King (2009) analyzed 10 short baseline (< 200m) with time series spanned several years calculated by TRACK software, among them 6 baselines appeared evident annual signal with amplitude >0.5mm and 2 have annual signals with amplitude even larger than 2mm. King (2010) calculated the effects of multipath on coordinate time series over several years of IGS stations using simulative method. The results indicated that time-variable biases of up to several millimetres are introduced in time series and the frequency and magnitude of this signal is dependent on site location and multipath source. Multipath effects propagate to the coordinates with the inversion of normal equations. The propagation mechanism relates to the least square design matrix that is controlled by the observation geometry, satellite constellation and local obstructions. As is known to all that the multipath effect can be weakened to a certain degree using the double differential solution. Besides, the multipath effect is dependent on the elevation angle of the satellite and its impact is more obvious if the elevation angle is lower. Therefore, the observation involved in this paper were processed for elevation cut-off angle of 15° and 25° respectively, Table 1 shows the difference of statistics between two solutions.

The time series from these different solutions are systematically offset from each other, which is true for all components, as shown in table 1. The offset for horizontal components is ~0.5mm, while for the radial is ~1mm. And the average RMS difference between two solutions is 0.4mm, 0.3mm and 1.0 mm for the north, east and vertical component respectively. Maximum RMS difference occurs in station S171 for radial component, while minimum difference occur in station L022 and TN01. There is no apparent periodic signal for the difference sequence of TN01 and S171 as seen in figure 2, which suggests that the time series are similar and periodic signal remain with similar amplitudes regardless of the different elevation angle cutoff used. It is inferred that multipath effect is not the major contribution of those signals in the monitoring stations. In addition, stations TN01, L022 have lowest difference between two solutions than other stations (largely due to their location. TN01 is located far away from the reservoir as a reference station; L022 is located in far side of the shore). While other stations such as S171 are located on the near waterside shore and have relatively higher multipath effect due to water surface reflection. Compared with TN01 shown in figure 3, there appeared a slight linear trend for north, east component and periodic signal for radial component in the difference sequence of S171 in figure 4, which implies some level of the influence due to multipath.

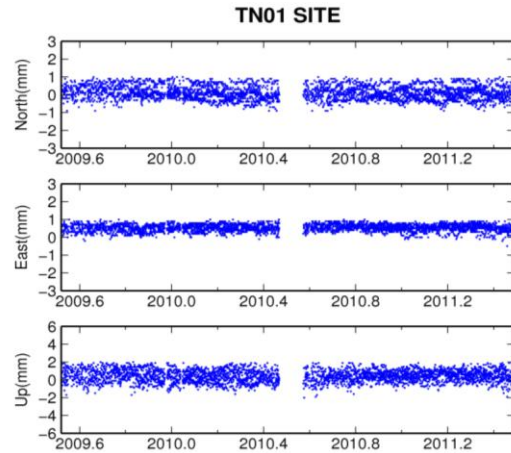


Figure 3. Difference sequence between solutions for 15° and 25° elevation cutoff angle for the monitoring stations TN01

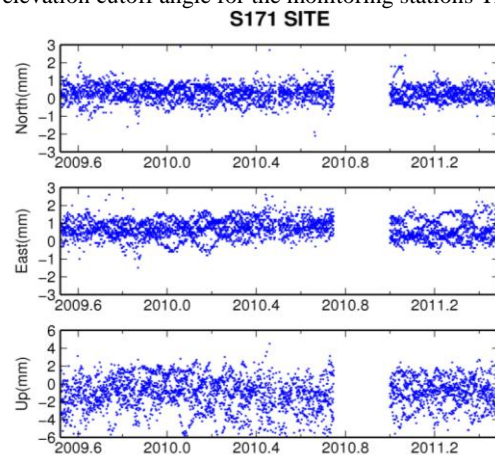


Figure 4. Difference sequence between solutions for 15° and 25° elevation cutoff angle for the monitoring stations S171

4.2. Fitted Model

Agnew and Larson (2007) analyzed the series by PPP and found that there exists periodic signals including annual, semiannual, diurnal (S1), semidiurnal (S2), ~K1 and ~K2 in the GPS coordinate time series. The ~K1 have a period of 1.03 d, which is the repeated cycle of the GPS satellite constellation, The ~K2 is the harmonic wave of K1, with a period being half of ~K1. Although it is well known that multipath introduces short-period (<10 min), ~K1 and its harmonics signal into GPS coordinate time series, we can ignore the influence of the multipath effect on long-term deformation in our time series according to above analysis. In this paper our time series was fitted with a model consisting of offset, secular and annual and semiannual terms.

For GPS short-baseline time series, the main error source are the multipath effect, PCV and the fluctuation due to instability of the observation pillar. Many researches showed that correlated noise is dominant in the long baseline time series, which can be best described by a combination of white noise plus flicker noise (Williams, 2009). Some investigations focused on the noise characteristics of GPS short-baseline. Nikolaidis (2002) obtained single epoch coordinate time series of one baseline (50m) with 12 weeks using the double differential method, the spectral index for the NEU components are -0.32, -0.35, -0.23 respectively through FFT analysis. The spectral index of short-baseline time series over 2.6 years

estimated by Hill (2009) is 1.4 ± 0.2 for north component, 1.5 ± 0.2 for east component and 0.9 ± 0.3 for vertical component. It seems that the spectral index in small-scale network solution is more varied due to the low level and undetermined mixture of local effects. There is no final conclusion for the noise characteristics of short-baseline time series until now and it still

needs further research. In order to obtain more reliable estimation of long-term deformation, in this paper we characterize the noise model in our time series with white noise (wn) and white noise plus flicker noise (wn + fn), which are raised mostly by previous researches.

Station	White Noise (mm/yr)			White Noise plus Flicker Noise (mm/yr)		
	North	East	Vertical	North	East	Vertical
L022	0.3 ± 0.03	1.9 ± 0.02	-3.8 ± 0.04	0.4 ± 0.20	2.2 ± 0.19	-3.9 ± 0.28
L132	-0.1 ± 0.04	-0.8 ± 0.03	-1.4 ± 0.05	-0.1 ± 0.36	-0.7 ± 0.15	-1.4 ± 0.19
S071	-0.5 ± 0.05	2.0 ± 0.12	-0.8 ± 0.06	-0.8 ± 0.37	2.3 ± 0.62	-0.9 ± 0.41
S171	-0.0 ± 0.05	-0.3 ± 0.04	-0.5 ± 0.07	-0.2 ± 0.37	0.1 ± 0.17	-0.3 ± 0.19
S191	0.0 ± 0.04	-0.2 ± 0.03	-1.0 ± 0.06	-0.0 ± 0.25	-0.0 ± 0.27	-0.9 ± 0.21

Table 2. Velocity estimates of white noise and white noise plus flicker noise for the north, east, and vertical components of the monitoring station in Xilongchi upper reservoir

Station	White Noise (mm)			White Noise plus Flicker Noise (mm)		
	North	East	Vertical	North	East	Vertical
L022	0.7 ± 0.02	0.8 ± 0.02	0.9 ± 0.02	0.6 ± 0.11	0.7 ± 0.11	0.8 ± 0.11
L132	0.6 ± 0.03	0.4 ± 0.02	0.4 ± 0.02	0.5 ± 0.18	0.3 ± 0.07	0.4 ± 0.18
S071	0.5 ± 0.04	1.1 ± 0.09	0.2 ± 0.04	0.8 ± 0.21	1.2 ± 0.60	0.3 ± 0.21
S171	0.2 ± 0.04	0.9 ± 0.04	0.6 ± 0.04	0.2 ± 0.23	0.8 ± 0.10	0.6 ± 0.13
S191	0.5 ± 0.03	1.0 ± 0.02	0.2 ± 0.03	0.5 ± 0.13	1.0 ± 0.14	0.2 ± 0.13

Table 3. Annual signal amplitude estimates of white noise and white noise plus flicker noise for the north, east, and vertical components of the monitoring station in Xilongchi upper reservoir

4.3. Secular and Annual Movement

The coordinates time series of each monitoring station in Xilongchi system is analyzed by CATS software (Williams, 2008). CATS is a program applying Maximum Likelihood Estimation to fit time series to a multi-parameter model. The routine solves all parameters simultaneously. The linear part includes an offset and slope, the possibility of abrupt steps and sinusoidal terms, while the non-linear part solves for several specific noise models and combinations. The estimated values of parameter including velocity and annual signal amplitude are shown in table 2 and table 3 respectively, and the corresponding noise model is confirmed as white noise and white noise plus flick noise.

For the two solutions, we find that the difference of estimated value in all components between two noise models is very small, which can even be neglected except the errors. It's obvious that the components are less noisy for white noise than white plus flicker noise. White noise is the preferred noise model for our time series. We can draw the same conclusion from the quantity of MLE, the calculated maximum log-likelihood value, which reflect the agreement between the time series and adopted model as an indicator in CATS. The MLE of white noise is much smaller than that of white noise plus flicker noise. It's inferred that white noise is dominant in stochastic signal compared with flicker and random walk noise owing to the

shorter span (2 years) and low sampling interval (4 hours) of our time series, which is different from previous investigation in which the sites were globally distributed, the noise can be best described by a combination of white noise plus flicker noise (Williams, 2004). It seems that we can attribute the white noise in short baseline to site-specific GPS errors such as multipath and PCV, another correlated noise source corrupts the medium-long baseline in which the most likely error are troposphere effects and errors related to orbit, atmosphere, ocean tide for long baseline (Nikolaidis, 2002)

The main movement tendency of stations in Xilongchi is comprehensible from the estimated parameters with white noise. As shown in figure 5 and figure 6, L022 site located in the main dam moves north by east 81° at 1.9 mm/yr , and S071, north by east 109° at 2.5 mm/yr , L132, north by west 87° at 0.8 mm/yr . Other sites such as S171 and S191 move slightly, the quantity is less than 0.3 mm/yr . All sites subside differently, among them L022 site exhibits strongest subsidence as high as 3.8 mm/yr , and L132 on auxiliary dam with a descending velocity of 1.4 mm/yr . The deformation of Xilongchi upper reservoir is revealed that the main dam moves eastward and the auxiliary move westward approximately. Meanwhile the whole reservoir subsides, the main and auxiliary dam appears more intense distortion compared with other section in vertical direction as well as horizontal direction.

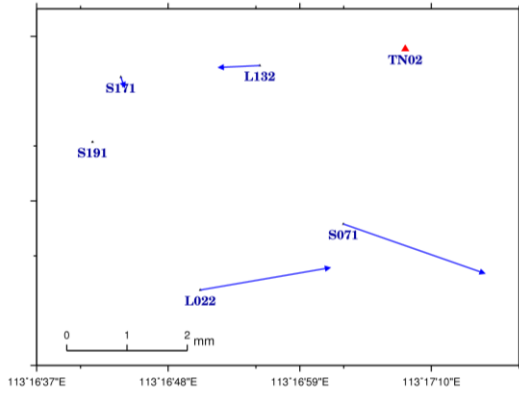


Figure 5. Horizontal velocities of GPS stations in Xilongchi upper reservoir

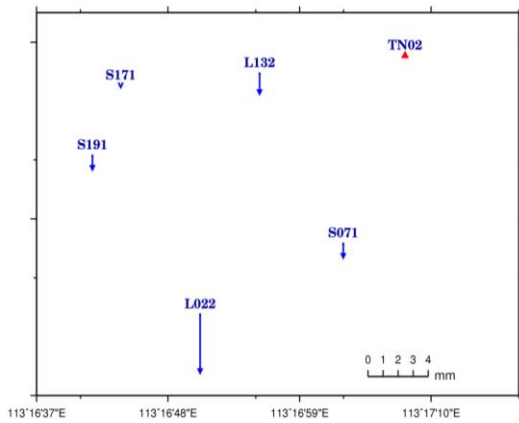


Figure 6. Vertical velocities of GPS stations in Xilongchi upper reservoir

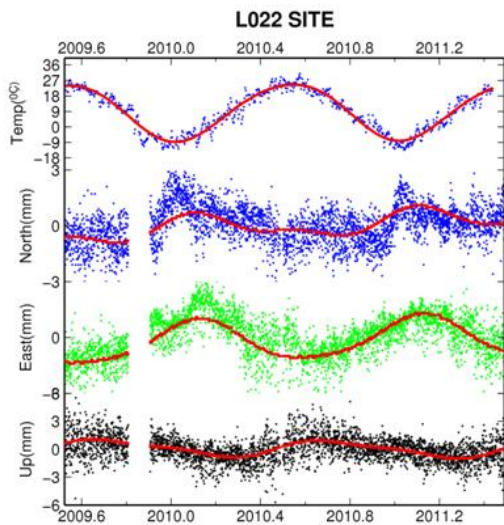


Figure 7. Seasonal cycle for temperature and coordinate time series for all components for station L022 after removing of secular signal of a model, the red lines represents the same data fitted by the model.

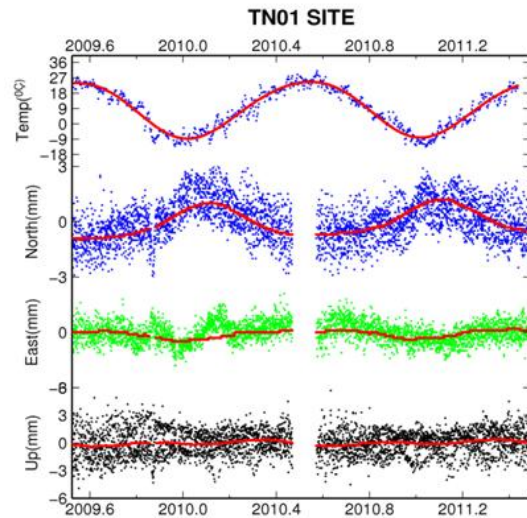


Figure 8. Seasonal cycle for temperature and coordinate time series for all components for reference station TN01 after removing of secular signal from a model, the red lines represent the same data fitted by the model.

It's revealed that there exists some difference between estimated annual amplitudes of north, east component of each monitoring stations as shown in table 2 in which the annual signal are more evident in N, E, U components for L022 and the east component for S071, S171, S191 and the amplitude was up to ~1mm. The difference is mainly in north component for L132 and the amplitudes is up to 0.5mm. All stations undergo a small level of displacement as shown in figure 2, which presents seasonal feature with peak in January and trough in May every year. There existed extreme relation between the signal in horizontal component of site L022, TN01 and local temperature as shown in figure 7 and figure 8. And the annual signal logs the local temperature by some days. This situation is much like the conclusion from King et al (2009), which suggested that seasonal cycles occur in the time series, with amplitudes $\leq 0.6\text{mm}$. Such signals existed even in horizontal component and for the shortest baseline. Seasonal cycle for time series have an lag up to 1 month after seasonal cycles in local temperature, with bedrock thermal expansion a possible cause". There is a reason to believe that the seasonal cycle for our time series are also related to bedrock thermal expansion although we did not calculate the lag time owing to the shorter span of observations. The consequence is inconsistent with our cognitions that the network is so small that the displacement can be cancelled as a common mode error. It is possible that there are still some unequal reactions of each station for the bedrock thermal, which can explain the contradiction. (WANG, 2005)

Further efforts to reliably model these signal are necessary and we leave this problem to be solved in future studies. However, it is certainly considered that linear movement as the dominant deformation in Xilongchi upper reservoir.

5. CONCLUSION

In this paper, we processed the continuous GPS observations of five monitoring stations in Xilongchi upper reservoir during 20 months and acquired the time series. Long-term deformation of the reservoir is determined and main conclusions are shown as follows.

- 1) We found that estimated parameters such as velocity and

amplitudes in the horizontal component are similar regardless of the different elevation angle cut-off used, which suggests that those quantities have elevation mask angle independence, and multipath is not a significant effect for them. There are no other errors left which will contribute both time- and space-dependent signal at a level of several millimetres in our time series. Therefore it is inferred that the secular signal represents the true movement of each monitoring station in Xilongchi upper reservoir.

2) Few significant differences can be found between the results of white noise and that of white plus flicker noise except the precession of estimated parameters. White noise is the preferred noise model for our time series through the comparison of the MLE value of CATS, which may be taken as evident that white noise is dominant in stochastic signal compared with flicker and random walk noise owing to shorter scale in our network.

3) The main and auxiliary dam of Xilongchi upper reservoir appears more intense linear deformation compared with other sections. It could be deduced from the analysis that 1) L022 site located in the main dam moves north by east 81° at 1.9mm/yr, while L132 in auxiliary north by west 87° at 0.8mm/yr. 2) L022 exhibits strongest subsidence as high as 3.7mm/yr, and L132 with a velocity of 1.2mm/yr. 3) Other sites such as S171 S191 moves slightly, and the quantity of velocity is less than 0.3mm/yr.

4) Annual signal are more evident in N, E, U components for L022 and the E component for S071, S171, S191 as the amplitude was ~ 1 mm. There is correlation between signal in horizontal component and local temperature, which suggests the cause of bedrock thermal expansion.

We have determined a long-term deformation tendency for Xilongchi upper reservoir from continuous GPS observations in this paper. Further research should focus on the establishment of theoretical model which integrates GPS monitoring results, hydrology, meteorological data. It will play a key role in revealing the deformation mechanisms of structures such as Dam.

References

- Agnew, D. C., and Larson, K. M., 2007. Finding the repeat times of the GPS constellation. *GPS Solut.*, 11(1), pp.71–76.
- Dong, D., P. Fang, Y. Bock, M. K. Cheng, and S. Miyazaki, 2002. Anatomy of apparent seasonal variations from GPS-derived site position time series. *J. Geophys. Res.*, 107(B4), 2075.
- Hill, EM., Davis JL., et al 2009. Characterization of site-specific GPS error using a short-baseline network of braced monuments at Yucca Mountain, southern Nevada. *J Geophys Res.*, 114(B11402).
- Jiang Weiping, Liu Jingnan, Ye Shirong, 2001. The Systematical Error Analysis of Baseline Processing in GPS Network. *Geomatics and Information Science of Wuhan University*, 26(3), pp.196-199. (in Chinese)
- King, M.A., Williams, S. D. P., 2009. Apparent stability of GPS monumentation from short-baseline time series. *J Geophys Res.*, 114(B10403).
- Nikolaïdis R., 2002. Observation of Geodetic and Seismic Deformation with the Global Positioning System. University of California, San Diego.
- Williams, S. D. P., 2008. GPS coordinate time series analysis software. *GPS Solut.*, 12, pp.147-153
- Williams, S. D. P., 2009. Error analysis of continuous GPS position time series. *J Geophys Res.*, 109(B03412).
- Wang Min, Shen Zhengkang, Dong Danan, 2005. Effects of non-tectonic crustal deformation on continuous GPS position time series and correction to them. *Chinese Journal of Geophysics*, 48(5), pp.1047-1052.